



Comparative study of quasi-static and dynamic behaviours of a reduced model of ASM4 rockfall barriers

Romain Boulaud, Cyril Douthe

► To cite this version:

Romain Boulaud, Cyril Douthe. Comparative study of quasi-static and dynamic behaviours of a reduced model of ASM4 rockfall barriers. IABSE's 40th Symposium on Tomorrow's Megastructures, Sep 2018, Nantes, France. 8p. hal-01934986

HAL Id: hal-01934986

<https://hal.science/hal-01934986>

Submitted on 26 Nov 2018

HAL is a multi-disciplinary open access archive for the deposit and dissemination of scientific research documents, whether they are published or not. The documents may come from teaching and research institutions in France or abroad, or from public or private research centers.

L'archive ouverte pluridisciplinaire **HAL**, est destinée au dépôt et à la diffusion de documents scientifiques de niveau recherche, publiés ou non, émanant des établissements d'enseignement et de recherche français ou étrangers, des laboratoires publics ou privés.



Comparative study of quasi-static and dynamic behaviours of a reduced model of ASM4 rockfall barriers

Romain Boulaud, Cyril Douthe

Laboratoire Navier – UMR 8205 – Ecole des Ponts Paris-Tech, IFSTTAR, CNRS

6 et 8 avenue Blaise Pascal – Champs sur Marne – 77455 Marne la Vallée CEDEX 2

Contact: romain.boulaud@enpc.fr

Abstract

ASM4 rockfall barriers is a protection device against the risk of rocks falls. These structures undergo large deformation and due to high geometrical and material non-linearities, the development and the use of computational tools are essential to carry out predictive approaches and optimise their design at reduced cost. In order to reduce considerably computation times, this paper presents an original approach, which consists of considering a reduced model of rockfall barrier comprising only few degrees of freedom rather than many thousands for a complete structure. The model is developed from the numerical simulations results carried out from a quasi-static experiment. After the accuracy of the model is verified with this first experiment, its potential to reproduce the real dynamic behaviour of a barrier is studied.

Keywords: reduced model, sliding cable, non-linear behaviour, dynamic relaxation.

1 Introduction

The hazard of landslide, mainly in mountain areas, compromises the safety of inhabitants. The need to protect them, their properties and infrastructures against this risk requires the installation of protective structures. Rockfall barrier is an often used alternative because of its low weight and its high capacity to absorb energy. It can be installed, by specialized workers, on hardly accessible zones. These kits have complex structures which can be described schematically as follows: a wire net (intercepting the block) supported by cables connected by steel posts to the cliff. The dissipation of the rock kinetic energy is insured by the net itself and by brakes distributed along the cables. The first section of this paper is dedicated to the modelling of a rockfall barrier. The second section presents the simulations of quasi-static experiment on a barrier prototype with a dynamic relaxation algorithm. The results of these simulations are then investigated to develop a simplified model of barrier whose accuracy is verified with the same

experiment. This model is then subjected to a dynamic loading and the comparison of its behaviour with a full scale experiment is conducted in the last section. Every experiments presented in this paper were carried out in the framework of the French national project C2ROP (www.c2rop.fr) which brings together many public and private partners around the topics of landslide risk and protection devices.

2 Rockfall barrier modelling

In this paper, we focus on the numerical modelling of two components: the support cables and the net. All modelled behaviours presented in this section are elastic.

2.1 The wire net

The wire net used for the barrier studied in this paper is an ASM4 ring net (see figure 1). It is an anti-submarine net in which each ring has four neighbours. This kind of net is widely used in

practice and many authors have proposed models to simulate its behaviour ([1], [2], [3]).

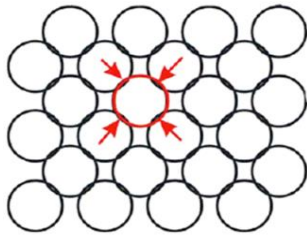


Figure 1. Pattern of ASM4 ring net

The behaviour of a ring is deduced from a plane tensile test on a net of 3 cells by 3 cells, whose results are presented in figure 2. It can be divided in two different stages. During the first stage only bending occurs without elongation of the ring perimeter, while in the second stage the constituent cable of the ring undergoes tensile stress. By assuming that the ring deformation is uniform in the square net, the tensile behaviour law of a single ring can be identified from the experimental results in the loading direction. This law is then continuously described thanks to the least squares method with a 5th degree polynomial. The modelled ring is a diamond whose vertices are the contact points with the four adjacent rings (see figure 1). Its initial length from which the strain is calculated is hence the perimeter of the square inside the circle of diameter d : i.e. $l_0 = 2\sqrt{2}d$.

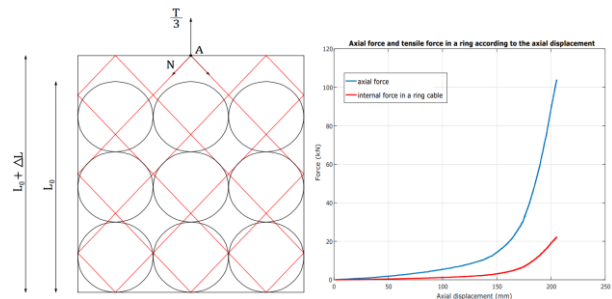
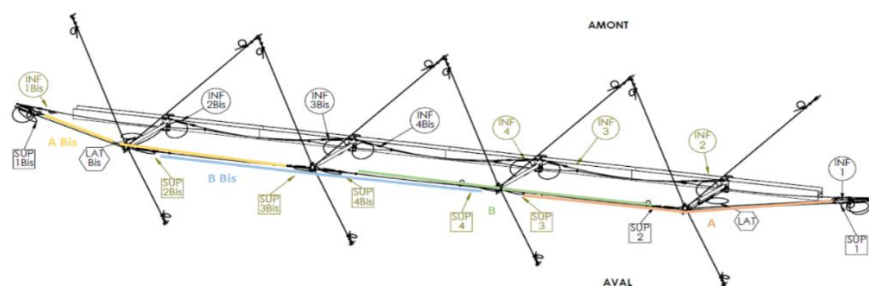


Figure 2. Experimental results of the plane tensile test

2.2 The support cables

When a block impacts the interception structure, the net slides along the support cables and tends to concentrate around the impacted zone. The geometric reorganization, created by the sliding of the net, allows to increase the motion (in the vertical direction) of the complete structure and minimise hence the forces in the structure. This phenomenon is called “curtain effect” and is commonly modelled with a “sliding cable”. Many models with or without friction have been developed and are available in the literature ([1], [4], [5]). The model used here does not take into account friction [6]. In practice these cables are currently linked with one or two energy dissipating devices which confers to the set formed by these two elements a bi-linear elastic-plastic behaviour.



(cables A and Abis on the figure 2) and two central cables connect the head of the first and the third posts (cable B and Bbis). Each cable holds partially the net and is free near the head of each post. With this assembly, the net is held by two cables in the centre of modulus and by a single cable near the posts. The net is of type ASM4 and is oriented as shown in Figure 1. It consists of 34 rings in the length direction and 8 rings in the height, each 27cm in diameter. The set formed by the net and the support cables is held to the cliff by 4 steel posts (modelled by beam elements). Moreover 3 cables (two upstream and one downstream), anchored in the cliff, hold the head of each post. Brake elements are connected in series with each support cable.

A quasi-static loading is applied to the structure. A 740 kg normalized polyhedral-shaped concrete block as specified in ETAG 027 [7] is maintained by a winch and slowly placed on the middle of the net until the barrier reaches equilibrium under dead-weight and block load. Then, another winch is hooked on the bottom part of the block and pulled orthogonally to the net. Its vertical displacement is controlled and slowly increased so that the loading might be considered as quasi-static.

3.2 Dynamic relaxation method

The dynamic relaxation is a discrete numerical method used to determine the equilibrium state of a system subjected to mechanical loads [8]. Its principle consists in linearizing the differential equation of the first Newton law by an explicit scheme of numerical integration. The static position of a structure is hence considered as the result of a smoothed dynamical process. If the forces are conservative the dynamical behaviour of the system has no influence on its equilibrium state. So the damping parameters may be chosen to optimize the convergence of the algorithm. In this paper an artificial damping proposed by P.Cundall and called "kinetic damping" is considered [9]. The numerical tool used in this study was developed in Laboratoire Navier for the study of structure in large displacement [10].

3.3 Comparison with the numerical simulation

During the experiment the resultant force applied to the winch is recorded by a load cell. In order to minimize the impact of local phenomena on the numerical results, we focus on the elastic energy which is integrated on the whole structure. This elastic energy is compared with the work of the resultant force applied to the winch, which has been numerically smoothed (see figure 4). The tensile forces in the central support cables are also compared (cables B and Bbis in figure 3). Since the real structure is not symmetric and different cell technologies have been used, an average of the forces in the upstream and downstream cables is compared with the numerical results (see figure 5). Even if the simulated behaviours of these cables does not correspond exactly to reality (difference of the initial stiffness), it can be considered that the numerical results are generally in good agreement with regard to both an overall and a local criterion. We can therefore have reasonable confidence in our numerical simulations and thus study more precisely the distribution of forces in the structure in order to propose a simplified model of this barrier.

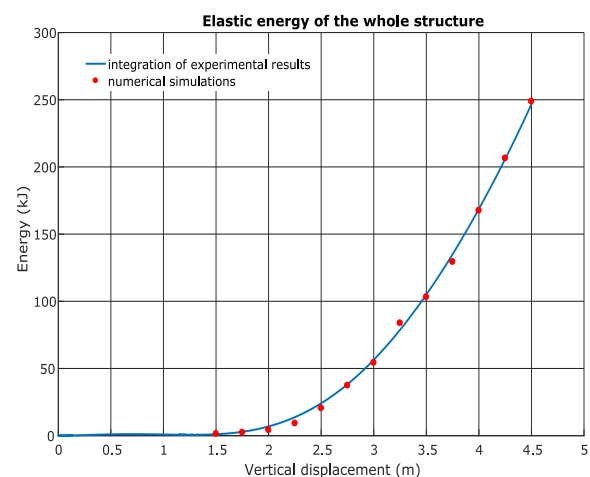


Figure 4. QS experiment vs numerical results

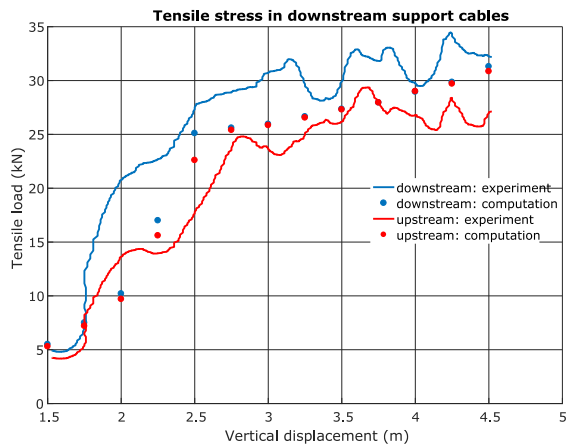


Figure 5. Central support cables behaviour: experiment vs numerical simulations

4 Development of a reduced rockfall barrier model

4.1 Geometry choice

To define the geometry of our model, we consider the deformed shape of our barrier for an axial deformation of 3,75 m, which corresponds to the moment when half of the final elastic energy of the structure is stored (see figure 6). The first assumption is to consider that the structure is completely symmetrical according to the two main directions of the net plane. Secondly, post head motions are assumed to be very small compared to the motions of other points in the structure.

Considering only the superstructure (i.e. the edge cables, since the displacement of the posts is neglected), the motion of the barrier is fully described by the displacements of the two points marked A and B in Figure 6. Considering only these degrees of freedom, it is still necessary to disregard the curvature of the edge cables at the central module.

To model the deformation of the net, it is chosen to follow the displacement of the lowest point of the structure located in the middle of the net (point C in figure 6). The vertical deformation of the net is thus given by the elongation of the BC segment. This degree of freedom is the only one added for the net. Indeed, the front view shows that outside the central modulus the net is contained in the same plane as the edge cables.

The complete behaviour of the structure shows that this geometry changes very little from a vertical displacement of 2m. Between 0 and 2m, the central support cables have not yet completely slipped and point B is not located in the centre of the net. To simplify the model as much as possible, we neglect the geometric changes due to the cable slip. Since this transformation is made without deformation, it has no influence in terms of energy. Moreover for symmetry reasons, only a quarter of the structure is studied in the rest of this paper.

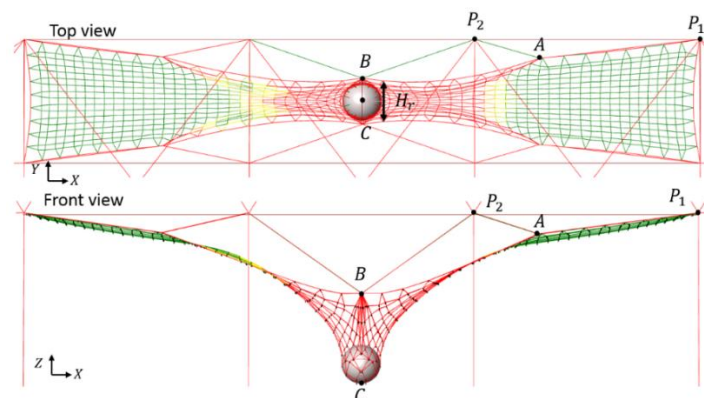


Figure 6. Distribution of internal forces in the structure for a vertical displacement of 3,75 m

4.2 Modelling internal efforts

4.2.1 Equilibrium of point A and B

The distribution of forces in the structure is shown in Figure 6 using a gradient of colours. Elements with a tensile stress of less than 0,5 kN are drawn in green while those with a tensile stress of more than 1 kN are drawn in red. It is thus observed that only the rings in the centre of the net are loaded so that the choice is made to apply a net-related stress only on the AB and BC segments. The other internal stresses in the modelled structure are related to the deformation of the support cables whose elastic-plastic behaviour has been described above. Figure 7 shows the reduced model and the different interactions taken into account.

According to the notations in Figure 7, the static equilibria of points A and B are fully described by the following system of equations:

$$\begin{cases} (T_1 + T_2)U_{AP_1} + (T_1 + T_{n2})U_{AB} + T_2U_{AP_2} = 0 \\ T_1U_{BP_2} + (T_1 + T_{n2})U_{BA} + T_{n1}U_{BC} = 0 \end{cases} \quad (1)$$

Where U-vectors designate the guiding vectors of considered segments. Note that the problem will be solved in 3 dimensions, but the drawings of the structure in top and front view are the same. T_1 and T_2 being the uniform tensile force in the centre and side edge cables and T_{n1} and T_{n2} the tensile stress associated with the net along the AB and BC segments respectively. All the interactions considered model cable behaviours, the elements of the simplified structure have thus no compression and bending stiffness.

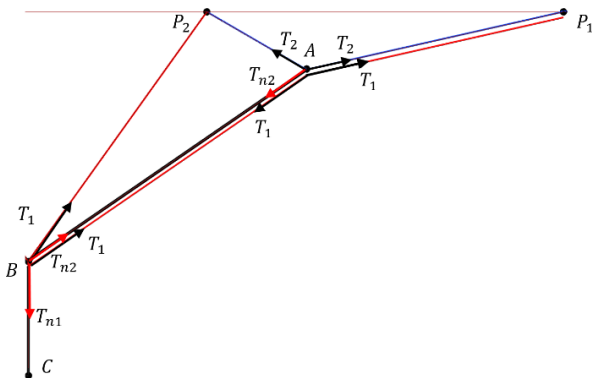


Figure 7. Reduced model of structure

4.2.2 Calculation of internal forces

Stress in the edge cables is calculated directly from the deformed geometry of the structure. By noting Δl_{lim} the limit deformation for which the stiffness of the assembly formed by the support cable and the brake element changes, the stress in a support cable is given by:

$$\begin{cases} T = K_0 \Delta l & \text{if } \Delta l < \Delta l_{lim} \\ T = K(\Delta l - \Delta l_{lim}) + K_0 \Delta l_{lim} & \text{if } \Delta l > \Delta l_{lim} \end{cases} \quad (2)$$

Where K_0 and K are respectively the stiffnesses before and after the limit deformation. The initial length is the same for the two cables: $l_0 = 10m$, and the limit deformation is given by the behaviour of the brake element. On the complete structure the cables are connected in series with a brake at each end. Equivalent stiffnesses and limit elongation of the cables are thus: $K_0 = 1190 \text{ kN}$, $K = 3600 \text{ kN}$ and $\Delta l_{lim} = 21 \text{ cm}$.

The difficulty is now to determine the behaviour of the two elements of the net from the ring behaviour that was established in the section 2.1. To simplify the reduced problem, the bending stage of the behaviour is not considered. The simplest way to describe these two efforts is thus given by the following relation:

$$\begin{cases} T = 0 & \text{if } l < l_{0,n} \\ T = K_n(l - l_{0,n}) & \text{if } l > l_{0,n} \end{cases} \quad (3)$$

Where K_n is the stiffness of the net element and $l_{0,n}$ its relaxed length. This two parameters must be calibrated from experimental results presented in section 3.3 for both net elements associated with AB and BC segments.

4.3 Fitting net properties with QS simulations

In order to determine the parameters (K_{n1} , $l_{0,n1}$, K_{n2} , $l_{0,n2}$), the quasi-static test presented in Section 3 is reproduced here. Loading in displacement is imposed by setting the altitude of point C. Since point B is fixed according to X, the problem has only 5 degrees of freedom. The equilibrium state of this system is solved with a

non-linear solver implemented in the software Matlab and using a trust-region algorithm [11]. This problem could be solved with the dynamic relaxation algorithm presented in section 2, but to facilitate the processing of the results, we prefer to use here this commercial scientific computation software. The resultant applied to the winch is hence compared with the force applied on the point C in the reduced barrier model for different vertical displacements.

Complete behaviours are calculated in this way for several sets of parameters determined from a 4th order Sobol series. Instead of approaching the results using an analytical response surface, the choice was here to densely map the parameters space and then determine the solution among the set of evaluation points. By noting \underline{X}_n the series of evaluation points, the solution is hence determined by means of the least square-method so that:

$$\underline{X}_S = \min_{\underline{X}_i} \sum_j [F_e(\delta_j) - F_{num}(\delta_j, \underline{X}_i)]^2 \quad (4)$$

In equation 4, \underline{X}_S is the vector grouping the best combination of parameters (K_{n1} , $l_{0,n1}$, K_{n2} , $l_{0,n2}$) among all \underline{X}_i tested. F_e and F_{num} are the forces measured experimentally and computed numerically respectively, while δ_j is the vertical displacement of the barrier (point C for the model). Identification results are presented in Table 1, and the numerical behaviour computed with these parameters is presented in figure 8.

Table 1. Net properties

K_{n1} (kN)	$l_{0,n1}$ (m)	K_{n2} (kN)	$l_{0,n2}$ (m)
4000	1,78	45	3,4

A change in behaviour of simplified model is observed for a vertical displacement of 2,25m. From this altitude, the force applied at point C increases linearly as a function of the displacement. The same phenomenon can be observed on experimental data for a vertical displacement of about 1,75m.

This behaviour change is due to the material non-linearity of sliding cables (see figure 9). It is possible

to identify 3 stages of the reduced model behaviour. In the first one the net deforms a lot without effort, in the second one (between 1,5 and 2,25 m) the length of the net almost no longer increases (high stiffness) and the support cable is activated. Finally for vertical block displacements greater than 2,25m the stiffness of the set composed by the cable and the brake elements change and the whole behaviour becomes linear.

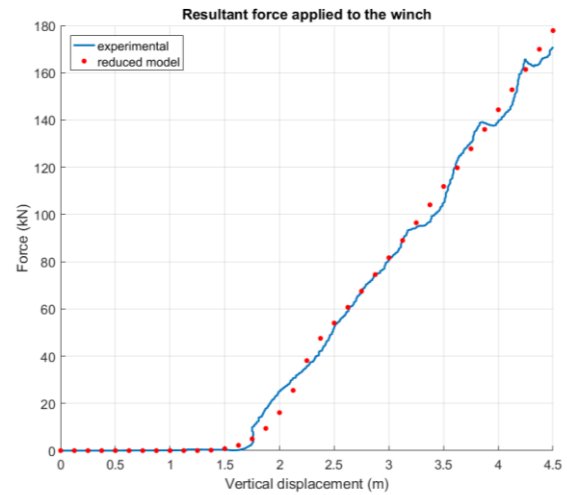


Figure 8. Simplified model behaviour

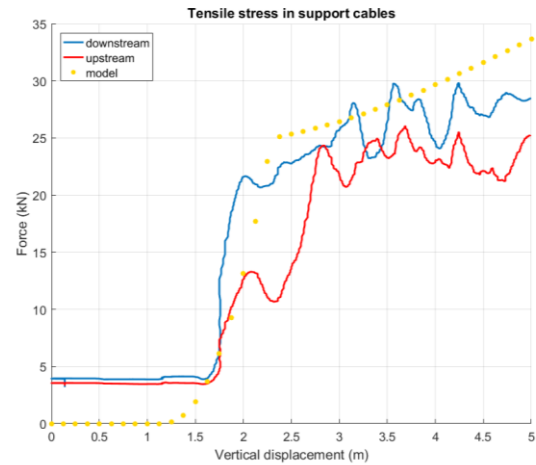


Figure 9. Support cables behaviour

Figure 9 shows the comparison between the evolutions of the tensile load in the support cables for the simplified model and the real structure. For the reduced model, the triggering of brakes occurs with a slight delay compared to the experiment.

For reasons of brevity, we will not further develop the study of the behaviour of this structure in quasi-static. However, we will note the potential of

simplified models to understand how efforts evolve in the structure. Now as the model is correctly calibrated and its performance has been validated in quasi-static, it can be tested under the dynamic loading regulated by ETAG27 and applied to rockfall barriers to certify their efficiency.

5 From Quasi-static to dynamic

5.1 Experimental device

The model response is compared to an experiment carried out in the framework of the C2ROP project and reproducing the conditions indicated by ETAG27 [10]. The barrier presented in Section 3 is impacted in the middle by a polyhedral boulder of 740 kg with a speed of 27m/s. This impact is repeated twice with two identical barriers. The acceleration of the block, its position and the tensile stress in some components are measured for both test during the whole impact period.

5.2 Calculation assumptions

The experimental results obtained during the two impacts reveal that the behaviour of the energy dissipating devices is different in quasi-statics and dynamics. The stiffnesses and the elastic limit given in the section 4.2.2 must thus be updated. The new values of these parameters are: $K_0 = 1190 \text{ kN}$, $K_b = 0 \text{ kN}$ and $\Delta l_{lim} = 16,8 \text{ cm}$. Moreover, the plastic dissipation due to the brakes is the only taking into account. The net elements are considered here perfectly elastic. A viscous damping representing the dissipation due to friction between elements in the real barrier is also introduced for nodes A and B. The problem has this time 6 ddl and is governed by the following system of equations:

$$\begin{cases} m_f \ddot{a}_A = (T_1 + T_2) \underline{U}_{AP_1} + (T_1 + T_{n_2}) \underline{U}_{AB} + T_2 \underline{U}_{AP_2} - C_A \underline{V}_A \\ m_f \ddot{a}_B = T_1 \underline{U}_{BP_2} + (T_1 + T_{n_2}) \underline{U}_{BA} + T_{n_1} \underline{U}_{BC} - C_B \underline{V}_B \\ m_b \ddot{a}_C = T_{n_1} \underline{U}_{CB} \end{cases} \quad (8)$$

The initial speed of all points is null except that of point C which is equal to -27m/s. The initial positions are given by the real barrier architecture, even if the initial position of point A has no influence on the barrier behaviour. The mass of the set formed by the net and the four support cables is estimated to be about 95 kg, which represents a

mass per nodes of 5,9 kg. Due to this difference between the masses, inertial forces will be concentrated in the block. The two damping coefficients are chosen equal to 10% of the critical damping associated with each node. Numerical integration is carried out using the explicit Runge-Khuta method of order 4 implemented in Matlab.

5.3 Comparison with the experiment

The response of the model to the impact described in section 5.1 is presented here and compared with the experimental results. We will focus here on the vertical trajectory of the block and the energy stored by the structure. Figure 10 presents the comparison of the block displacement between the model and the experiments. We observe that the numerical results are in good agreement with the experiments, even if the maximum elongation is reached with a slight delay: 0,28 s for the model against 0,25 s and 0,27 s for the first and the second impacts respectively.

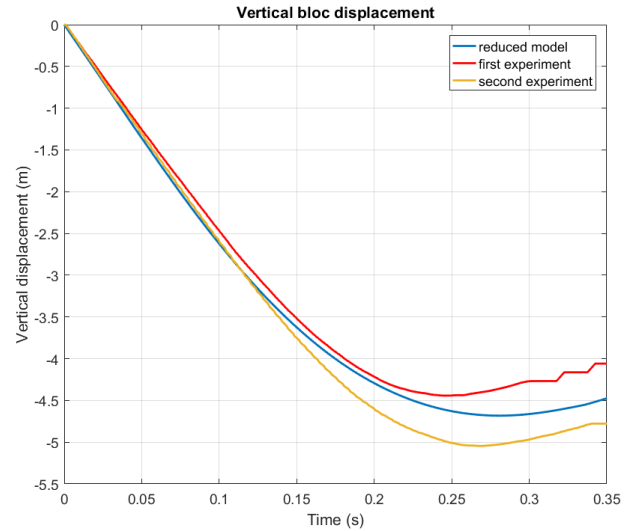


Figure 10. Block vertical displacement

The energy dissipated by the structure is calculated in each case by integrating the resultant force applied to the block. For the experiments this force is deduced from the vertical acceleration of the block.

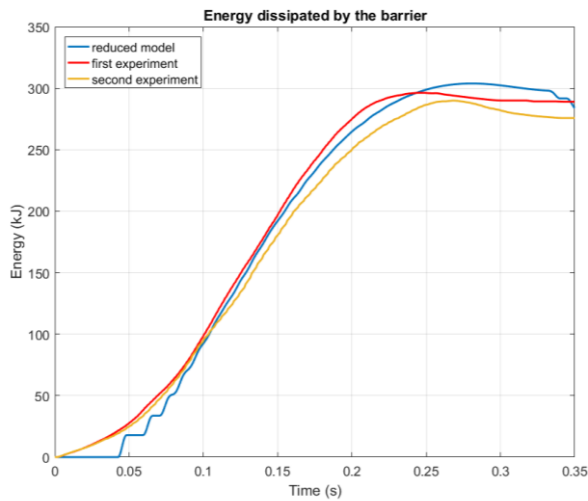


Figure 11. Energy dissipated by the barrier

The overall shape of the curve is in good agreement with experimental results although the dissipated energy is a little overestimate by the reduced model. We observe also a delay due to the modelling of the net interaction. Unlike the quasi-static behaviour, the structure is this time immediately loaded. The plates of energy which appear at the beginning of the impact for the reduced model are due to the gradually damped oscillations of point B caused by the sudden tensioning of the net element BC.

6 Conclusion

We showed in this paper that simple assumptions can be used to accurately reflect the overall dynamic behaviour of a rockfall barrier. However, there are still some limitations to use such models. Firstly, the behaviour of the net is not defined a priori. The stress distribution in the net should be more precisely investigated to define analytically equivalent behaviour. Secondly, by concentrating the net masses in two nodes we change the dynamical behaviour of the structure, even if this new distribution should not have a significant impact on the total energy dissipated by the barrier. Further development will be hence dedicated to better take into account dissipative phenomena such as friction and plasticity. Another work could also be dedicated to models off-centre impacts.

7 Acknowledgements

The experiments presented in this paper were carried out in the framework of the French national project C2ROP. The authors wish to thank all the members of the national project and particularly the members of the working group on soft barrier for their invaluable support, which allows for the achievement of this work.

8 References

- [1] Grassl H, Bartelt P, Volkwein A, Wartmann S. Experimental and Numerical Modeling of Highly Flexible Rockfall Protection Barriers.
- [2] Nicot F. Etude du comportement mécanique des ouvrages souples fr protection contre les éboulements rocheux. Centrale Lyon; 1999.
- [3] Coulibaly JB, Chanut M-A, Lambert S, Nicot F. Nonlinear Discrete Mechanical Model of Steel Rings. J Eng Mech [Internet]. 2017;143(9):4017087.
- [4] Coulibaly JB, Chanut M-A, Lambert S, Nicot F. Sliding cable modeling: An attempt at a unified formulation. Int J Solids Struct [Internet]. 2018;130–131:1–10.
- [5] Ghossoub L. Analyse de quelques éléments du comportement des écrans de filets pare-blocs. Université Paris Est; 2015.
- [6] Boulaud R, Douthe C, Ghossoub L, Sab K. Modeling of curtain effect in ASM4 rockfall barrier with the dynamic relaxation.
- [7] European Organisation for Technical Approvals Europäische. Etag 027. 2013.
- [8] Day A. An Introduction to Dynamic Relaxation. Eng. 1965;218–21.
- [9] Cundall P. A computer model for simulating progressive large scale movements in block rock systems. In: Symposium International of the Society of Rock Mechanics. 1971.
- [10] Douthe C, Baverel O. Design of nexorades or reciprocal frame systems with the dynamic relaxation method. Comput Struct [Internet]. 2009;87(21–22):1296–307.
- [11] More J, Sorensen D. COMPUTING A TRUSTREGION STEP. Soc Ind Appl Math. 1983;4(3):553–72.